

Chordae tendineae in Animal Models

Subjects: Veterinary Sciences

Contributor: Justyn Gach

Myxomatous mitral valve disease (MMVD) is the most common canine heart disease in which, among other things, chordae tendineae rupture occurs. The Chordae tendineae (CT) are part of the atrioventricular apparatus. They are mainly responsible for the mechanical functions of heart valves. In our study we performed biomechanical and histopathological examination of CT in order to better understand the functioning of the valvular apparatus. It is clinically relevant to begin further studies about biomarkers suggesting an episode of CT rupture, as such an episode leads to acute pulmonary oedema and worsens the clinical status of the patient.

Keywords: Chordae tendineae ; heart ; canine ; swine ; biomechanics

1. Introduction

The left atrioventricular apparatus is located between the left atrium and the left ventricle and consists of the following: mitral ring, anterior and posterior cusps, *Chordae tendineae*, and papillary muscles ^[1]. *Chordae tendineae* (CT) are columnar structures found only in mitral and tricuspid valves. CT are divided into three groups: first-order CT, which connect the leaflets and the papillary muscles, second-order CT located between the midventricular surface of both cusps and the papillary muscles, and third-order CT, which extend between the parietal leaflet and the ventricular wall ^{[2][3]}. The CT modulate the transmission of strain from the papillary muscles to the valve leaflets, as evidenced by the heterogeneity of the mechanical properties and structure of the chordal areas of adhesion on the leaflet ^[4]. The area of the valve leaflet without CT insertion regions is circumferentially stiffer than the area with CT attachments. In normal CT, the orientation of collagen fibres is complex throughout the area of the insert. This enables the three-dimensional transmission of strain through the CT ^[5].

Myxomatous mitral valve disease (MMVD) is the most common acquired cardiovascular disease in dogs, and accounts for approximately 75% of cases of chronic heart failure ^{[6][7][8][9]}. The etiology of the myxomatous process is still unknown ^[10]. Myxomatous mitral valves are characterized by a disorganization of the structural elements of the leaflets and a weakening of the *Chordae tendineae* as well. These changes cause a significant loss of the valve's mechanical properties, and often lead to valve prolapse and/or mitral regurgitation. In myxomatous mitral leaflets, collagen and glycosaminoglycan accumulation is observed ^[5]. This degenerative process also affects the CT ^[10]. The American College of Veterinary Internal Medicine (ACVIM) distinguishes four stages of MMVD. Stage A includes breed-predisposed dogs (e.g., Cavalier Kings Charles Spaniel, Yorkshire terrier, Maltese, Chihuahua, Dachshund) at high risk for developing heart failure in the future. Such patients show no clinical signs and no structural changes in the heart during the echocardiography examination. Stage B1 includes dogs without clinical signs but with a heart murmur present due to mitral regurgitation secondary to mitral valve leaflet degeneration, without enlargement of the heart chambers. Stage B2 includes dogs with structural heart disease (chamber enlargement). Stage C includes patients with current left ventricular heart failure symptoms or a history of such symptoms (exercise intolerance, cough, tachypnoe, dyspnea). Patients who have developed heart failure and present with recurrent heart failure symptoms despite standard treatment are classified as stage D. In stages C and D, a number of complications such as *Chordae tendineae* rupture, development of pulmonary hypertension and left atrial tear can occur ^[11].

The prevalence and progression of MMVD is strongly associated with age, breed and gender ^{[8][12][13]}. It occurs more often in small breeds than in large breeds. Males seem to be more vulnerable than females and can develop MMVD earlier ^{[14][15]}. The disease usually progresses over many years and morbidity is dependent on valve regurgitation and volume overload ^[16]. MMVD is recognized during auscultation of a heart murmur. A left apical holosystolic murmur is typical of mitral regurgitation ^[17]. However, definitive diagnosis is made by performing an echocardiographic exam. During this examination, it is possible to see changes in the valves (nodular and thickened appearance), enlargement of the heart chambers, and valve regurgitation ^[11].

The changes in leaflet composition and mechanics due to progressive degeneration are already known but, to the authors' knowledge, histological and mechanical changes in CT have not yet been evaluated in dogs. In our studies, we examined the biomechanical and structural characterisation of canine and porcine CT and the correlation between those properties. We evaluated the hypothesis that the histological and structural remodelling of CT (in addition to the valve leaflets) has an influence on the mechanical characteristics of CT and can contribute to a higher probability of CT rupture.

2. The Biomechanical Examination

During the biomechanical examination force–elongation characteristics were obtained and converted into strain and stress (Figure 1), determining the basic mechanical parameters such as tensile strength and Young's modulus.

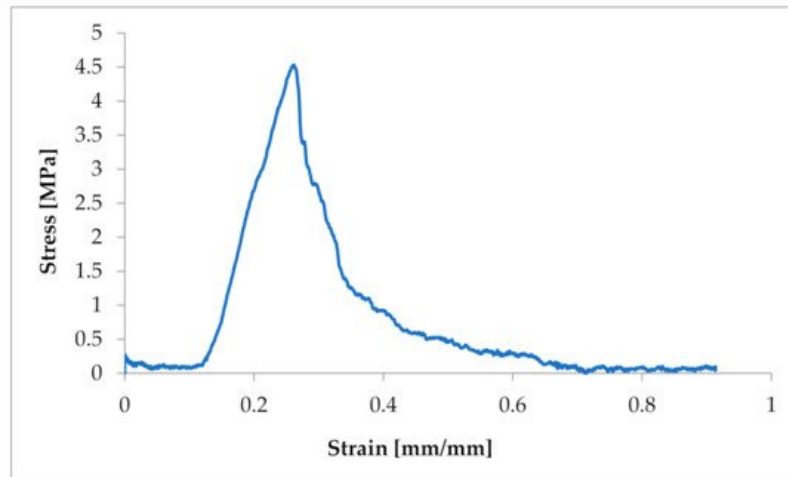


Figure 1. Example of a strain–stress ratio curve in one CT from a dog suffering from MMVD.

The obtained characteristics showed a strong non-linear character of the tensile response of *Chordae tendineae*. The shape of the curve showed a hyper-elastic model of this soft tissue material. It is worth mentioning that the curves were heterogeneous and showed a loss of stability when certain values of tensile force were exceeded. This shows the complex structure of the string and the arrangement of the fibres in bundles. When the strength of individual fibres was exceeded, there was a momentary decrease in strength, so the curve showed a decrease and then an increase to the strength of the next stretched fibre, etc. The maximum strength of a chorda tendinea is described by the breaking point of the strongest fibre. At the same time, the stretch diagrams showed micro-creeping, characteristic of soft tissues, which should be explained in more detail, together with the determination of the exact mathematical model of the tissue endurance of *Chordae tendineae*. This creep is related to the structure of the connective tissue that builds up the CT, which consists of elastin and collagen fibers that change their configuration inside the matrix during load application and removal.

The samples were tested at random, hence the large dispersion in the obtained values of tensile strength. In the case of pigs, the tensile strength had values of 3.19–12.419 MPa (average 7.522 ± 3.6 MPa). In the case of *Chordae tendineae* from healthy dogs, the tensile strength varied from 4.61 to 23 MPa (average 10.86 ± 5.60 MPa). Significantly lower strength values were observed for *Chordae tendineae* affected by the degenerative process. The highest value of the obtained tensile strength in these samples did not exceed 5.5 MPa and the determined average was 3.36 ± 1.88 MPa. Statistically significant differences were observed between healthy and degenerated CT ($p = 0.022$). Comparison of the CT from healthy dogs and pigs revealed no statistically significant differences between them ($p = 0.15$). Examples of strain–stress ratio curves for a healthy dog and a dog with degenerated *Chordae tendineae* are shown in Figure 2.

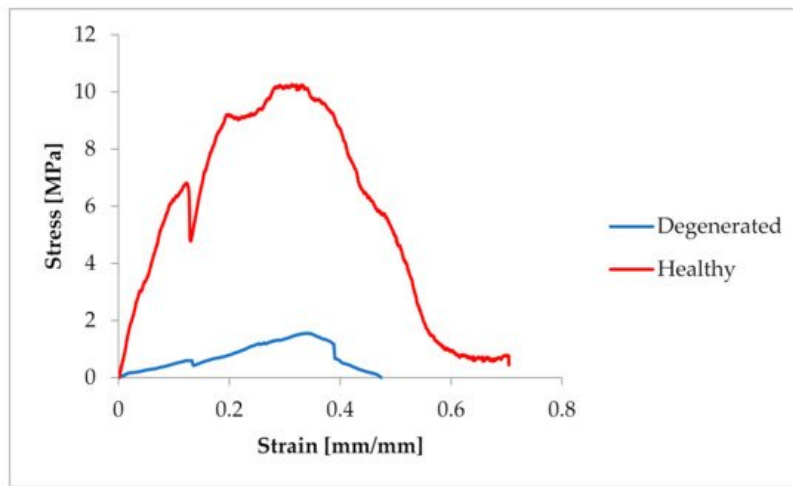


Figure 2. Comparison of the strain–stress ratio curve in healthy and degenerated CT.

3. Comparison of CT from Mitral and Tricuspid Valve

The average tensile strength value of the CT from the mitral valve was 13.96 ± 9.66 MPa, while that of the CT from the tricuspid valve was 3.6 ± 3.67 MPa. The differences are shown in Figure 3.

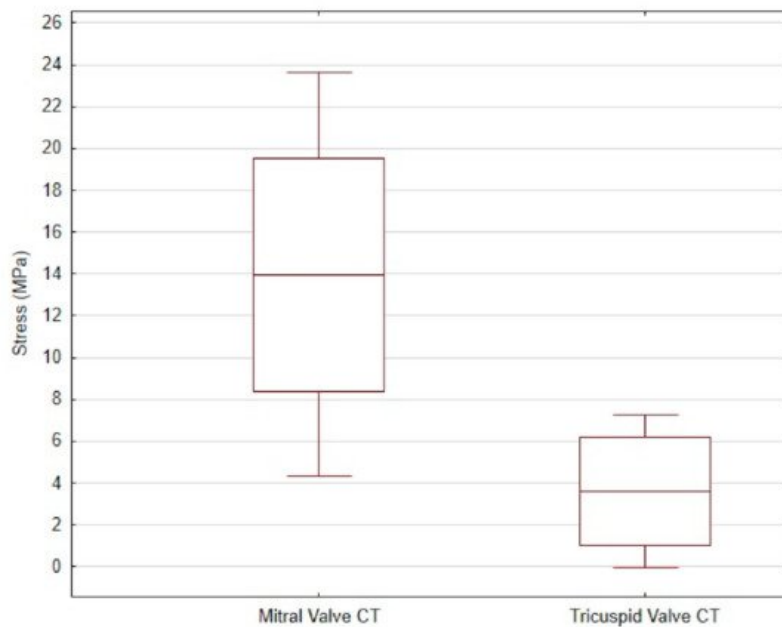


Figure 3. The mean and standard deviation of the stress values in the mitral valve CT and the tricuspid valve CT of dogs.

In order to determine the strength values of the *Chordae tendineae*, nonlinear stress–strain relationships for plot models and polynomial regression plots were developed at a parameter level of $R^2 \geq 86.3$. The strength values take elastic standard errors into account. The measurement error of the testing machine was ± 0.04 N, while the linear measurements from the digital images were accurate to 1 pixel.

4. The Histopathological Examination

The histopathological examination of the CT showed differences in structure between animals with normal valves and those suffering from mitral valve disease. The *Chordae tendineae* obtained from pigs and dogs with normal mitral valves showed a regular structure. The fibres were arranged collaterally, and the CT were regular in shape and diameter. In contrast, during mitral valve disease, the layout of connective tissue fibres became chaotic and disarranged. The elastic fibres showed segmental absence in the affected CT. Moreover, the *Chordae tendineae* from animals suffering from mitral valve disease showed segmental thickening (Figure 4 and Figure 5).

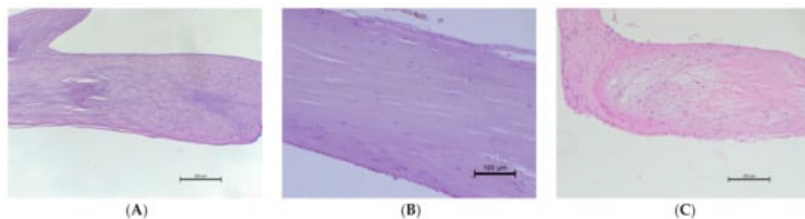


Figure 4. The microscopic examination of *Chordae tendineae* from normal and diseased mitral valves. **(A)** Normal chorda tendinea from pig; HE stain; magnification 40×. **(B)** Normal chorda tendinea from a dog; HE stain; magnification 200×. **(C)** Altered chorda tendinea from dog suffering from mitral valve disease—disarrangement in the filaments is visible; HE stain; magnification 100×. The left side of each figure is the attachment point to the valve, the right side is that to the papillary muscle.

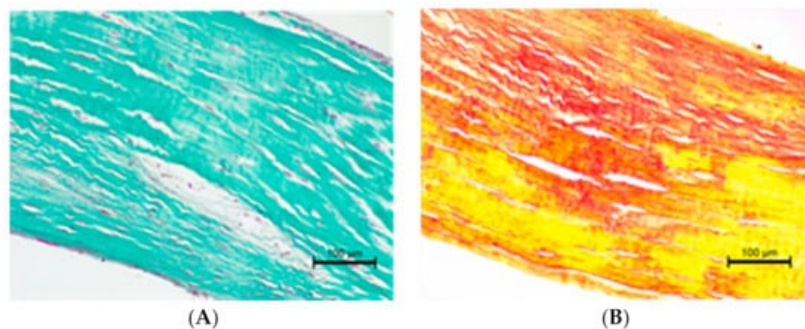


Figure 5. **(A)** Altered chorda tendinea from dog suffering from mitral valve disease—disarrangement in collagen filaments is visible; Masson–Goldner trichrome stain; magnification 200×. **(B)** Altered chorda tendinea from dog suffering from mitral valve disease—disarrangement and absence of elastic filaments in some parts of the tissue is visible; elastic red–picrosirius stain; magnification 200×. The orientation is the same as in Figure 4.

We also performed a histopathological examination of a ruptured CT. The structure was completely torn, with free spaces between the fibre bundles visible (Figure 6 and Figure 7).

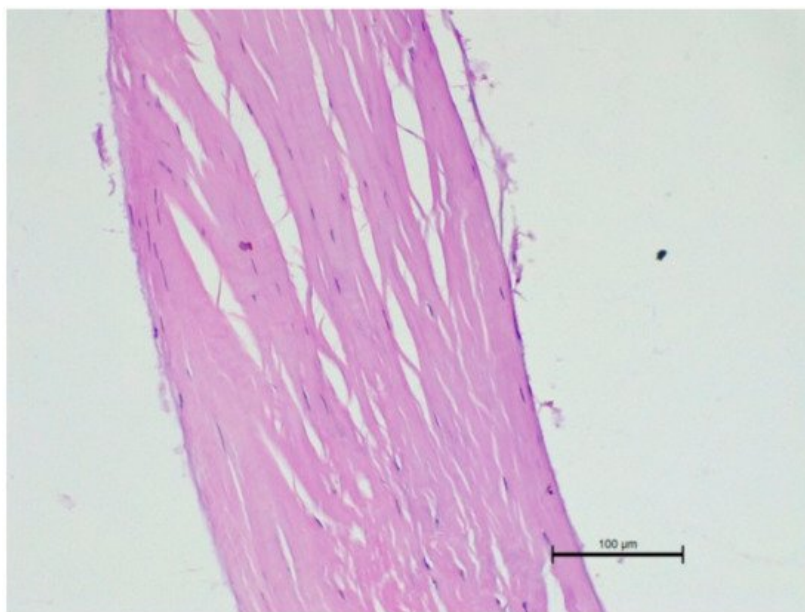


Figure 6. Microscopic examination of a ruptured chorda tendinea from a dog. A severe disarrangement of filaments is visible. HE stain; magnification 200×. Valve side is at the bottom of Figure, while the papillary muscle part is at the top.

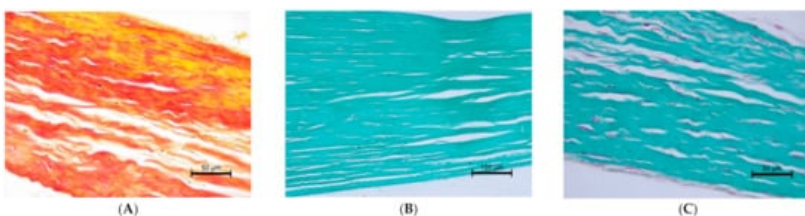


Figure 7. Ruptured *Chordae tendinae*. (A) elastic red–picrosirius stain; magnification 400×. (B) (magnification 200×) and (C) (400×) Masson–Goldner trichrome stain. The valve part is at the left and papillary muscle part at the right of each Figure.

References

1. Gunnal, S.A.; Wabale, R.N.; Farooqui, M.S. Morphological study of chordae tendinae in human cadaveric hearts. *Heart Views Off. J. Gulf Heart Assoc.* 2015, 16, 1–12.
2. Serres, F.; Chetboul, V.; Tissier, R.; Sampedrano, C.C.; Gouni, V.; Nicolle, A.P.; Pouchelon, J.L. Chordae tendinae rupture in dogs with degenerative mitral valve disease: Prevalence, survival, and prognostic factors (114 cases, 2001–2006). *J. Vet. Intern. Med.* 2007, 21, 258–264.
3. Morse, D.E.; Hamlett, W.C.; Noble, C.W. Morphogenesis of chordae tendinae. I: Scanning electron microscopy. *Anat. Rec.* 1984, 210, 629–638.
4. Ross, C.J.; Zheng, J.; Ma, L.; Wu, Y.; Lee, C.H. Mechanics and Microstructure of the Atrioventricular Heart Valve Chordae Tendinae: A Review. *Bioengineering* 2020, 7, 25.
5. Richards, J.M.; Farrar, E.J.; Kornreich, B.G.; Moïse, N.S.; Butcher, J.T. The mechanobiology of mitral valve function, degeneration, and repair. *J. Vet. Cardiol. Off. J. Eur. Soc. Vet. Cardiol.* 2012, 14, 47–58.
6. Borgarelli, M.; Haggstrom, J. Canine degenerative myxomatous mitral valve disease: Natural history, clinical presentation and therapy. *Vet. Clin. N. Am. Small Anim. Pract.* 2010, 40, 651–663.
7. Darke, P.G. Valvular incompetence in cavalier King Charles spaniels. *Vet. Rec.* 1987, 120, 365–366.
8. Detweiler, D.K.; Patterson, D.F. The prevalence and types of cardiovascular disease in dogs. *Ann. N. Y. Acad. Sci.* 1965, 127, 481–516.
9. Buchanan, J.W. Chronic valvular disease (endocardiosis) in dogs. *Adv. Vet. Sci. Comp. Med.* 1977, 21, 75–106.
10. Menciotti, G.; Borgarelli, M. Review of Diagnostic and Therapeutic Approach to Canine Myxomatous Mitral Valve Disease. *Vet. Sci.* 2017, 4, 47.
11. Keene, B.W.; Atkins, C.E.; Bonagura, J.D.; Fox, P.R.; Häggström, J.; Fuentes, V.L.; Oyama, M.A.; Rush, J.E.; Stepien, R.; Uechi, M. ACVIM consensus guidelines for the diagnosis and treatment of myxomatous mitral valve disease in dogs. *J. Vet. Intern. Med.* 2019, 33, 1127–1140.
12. Detweiler, D.K.; Luginbuhl, H.; Buchanan, J.W.; Patterson, D.F. The natural history of acquired cardiac disability of the dog. *Ann. N. Y. Acad. Sci.* 1968, 147, 318–329.
13. Das, K.M.; Tashjian, R.J. Chronic mitral valve disease in the dog. *Vet. Med. Small Anim. Clin.* 1965, 60, 1209–1216.
14. Fox, P.R.; Sisson, D.; Moise, N.S. *Textbook of Canine and Feline Cardiology. Principles and Clinical Practice*, 2nd ed.; WB Saunders: Philadelphia, PA, USA, 1999; pp. 536–565.
15. Olsen, L.H.; Martinussen, T.; Pedersen, H.D. Early echocardiographic predictors of myxomatous mitral valve disease in Dachshunds. *Vet. Rec.* 2003, 152, 293–297.
16. Fox, P.R. Pathology of myxomatous mitral valve disease in the dog. *J. Vet. Cardiol. Off. J. Eur. Soc. Vet. Cardiol.* 2012, 14, 103–126.
17. Pedersen, H.D.; Häggström, J.; Falk, T.; Mow, T.; Olsen, L.H.; Iversen, L.; Jensen, A.L. Auscultation in mild mitral regurgitation in dogs: Observer variation, effects of physical maneuvers, and agreement with color Doppler echocardiography and phonocardiography. *J. Vet. Intern. Med.* 1999, 13, 56–64.